Geosci. Model Dev., 5, 829–843, 2012
www.geosci-model-dev.net/5/829/2012/
doi:10.5194/gmd-5-829-2012

Geoscientific Model Development

GEWEX Cloud System Study (GCSS) cirrus cloud working group: development of an observation-based case study for model evaluation

H. Yang[1,2], **S. Dobbie**[2], **G. G. Mace**[3], **A. Ross**[2], **and M. Quante**[4]

[1]CMA Key Laboratory for Atmospheric Physics and Environment, Nanjing University of Information Science and Technology, no. 219 Ningliu Road, Nanjing, 210044, China
[2]School of Earth and Environment, Institute for Climate and Atmospheric Science, University of Leeds, Leeds LS2 9JT, UK
[3]Meteorology Department, University of Utah, 135 S 1460 East Rm 819 (WBB), Salt Lake City, UT 84112-0110, USA
[4]Helmholtz-Zentrum Geesthacht, Institute of Coastal Research/System Analysis and Modelling, Max-Planck-Strasse 1, 21502 Geesthacht, Germany

Correspondence to: H. Yang (huiyi.yang@physics.ox.ac.uk)

Received: 16 September 2011 – Published in Geosci. Model Dev. Discuss.: 24 October 2011
Revised: 18 April 2012 – Accepted: 20 April 2012 – Published: 8 June 2012

Abstract. The GCSS working group on cirrus focuses on an inter-comparison of model simulations ranging from very detailed microphysical and dynamical models through to general circulation models (GCMs). The past GCSS cirrus cloud inter-comparison highlighted the wide range in modelling results that was a surprise to the modelling community. That inter-comparison was idealised and, therefore, a key issue was that it did not benefit from observations to help distinguish between model performances.

In this work, we aim to address this key issue by developing an observationally based case study to be used for the GCSS cirrus modelling inter-comparison study. We focused on developing a case that had sufficient observations with which to evaluate models, to help identify which models in the inter-comparison are performing well and highlight areas for model development. Furthermore, it will provide a base case for future model comparisons or testing of new or updated models. This paper outlines the modelling case development and the inter-comparison results will be presented in a follow-on paper.

The case was based on the 9 March 2000 Atmospheric Radiation Measurement (ARM) Southern Great Plains (SGP) during an intensive observation period (IOP). The case was developed utilising various observations including ARM SGP remote sensing including the MilliMeter Cloud Radar (MMCR), radiometers, radiosondes, aircraft observations, satellite observations, objective analysis and complemented with results from the Rapid Update Cycle (RUC) model as well as bespoke gravity wave simulations used to provide the best estimate for large scale forcing. The retrievals of ice water content, ice number concentration and fall velocity provide several constraints to evaluate model performances. Initial testing of the case has been reported using the UK Met Office Large Eddy Simulation Model (LEM) which suggests the case is appropriate for the model inter-comparison study. To our knowledge, this case offers the most detailed case study for cirrus comparison available and we anticipate this will offer significant benefits over past comparisons which have mostly been loosely based on observations.

1 Introduction

The Global Energy and Water Cycle Experiment (GEWEX) Cloud System Study Programme (GCSS) was initiated by K. Browning and others in 1990. The purpose of GCSS is to develop better parameterizations of cloud systems within climate and numerical weather predication models (Randall et al., 2000). There were five initial Working Groups focusing on different clouds: boundary-layer clouds, cirrus clouds, extra-tropical layer cloud systems, precipitating

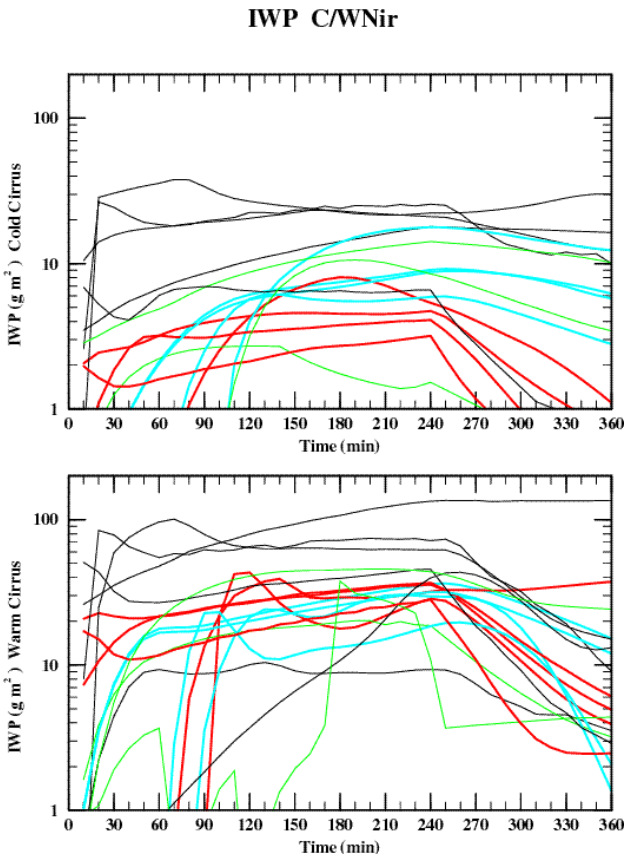

Fig. 1. Time series of vertically-integrated ice water path ($g\,m^{-2}$) from cirrus models, which participate the ICMCP. These baseline simulations correspond to night-time (infrared radiation only). The upper panel is for the "cold" (about $-66\,^{\circ}C$) cirrus case and the bottom one is for the "warm" (about $-47\,^{\circ}C$) cirrus case. A $3\,cm\,s^{-1}$ uplift is continuously applied over a 4 h time period and then there is a 2-h dissipation time. The colour cyan represents CSMs with bin microphysics, red represents CSMs with bulk microphysics, green represents single column models and the thin black represents CSMs with heritage in the study of deep convection or boundary layer clouds. This figure illustrates the wide range in cirrus model predictions for an idealised case (figure is taken from Starr et al., 2000).

deep convective cloud systems and polar clouds. This has been more recently extended to include other case developments such as Pacific Cross-section Intercomparison, etc. The cirrus working group (WG2) in the past has initiated one previous project focusing on high resolution cloud model inter-comparison. It was denoted the Idealised Cirrus Model Comparison Project (ICMCP) and had 16 models involved in the comparison ranging from cloud scale models (CSMs) to single column models (SCMs) (both GCM SCMs as well as highly detailed 1-D models).

The results of the first inter-comparison (ICMCP) were a surprise to the cirrus community. It showed that the community's numerical models of cirrus showed significantly larger disagreement than expected concerning such fundamental quantities as ice water path (IWP) for even idealised cases. The results appeared only in a conference paper (Starr et al., 2000). Figure 1 is taken from that paper and illustrates the range in results of as much as two orders of magnitude in IWP. There was some separate grouping noted between bin and bulk models, however, the range was large for all categories. The results from SCMs span the whole range of CSM results and models not originally developed for cirrus exhibit larger scatter and generally there was larger scatter for all model categories for the cold case.

In addition to the ICMCP inter-comparison, there was also a Cirrus Parcel Model Comparison Project (CPMCP) (Lin et al., 2002) which was a follow-on project as part of the GCSS WG2. The main aim of their study was to compare the microphysics specification of different cirrus models under idealised conditions. For complete details, refer to Lin et al. (2002).

Although well instrumented sites such as ARM provide significant amounts of data for modelling studies, developing a high-resolution modelling case based in observations is somewhat rare in the literature. Several studies have based their modelling studies on observations such as Brown and Heymsfield (2001) used TOGA-COARE data, Benedetti and Stephens (2001) used ARM data, Cheng et al. (2001) used FIREII data, Marsham and Dobbie (2005) and Marsham et al. (2006) used Chilbolton data, Solch and Karcher (2011) used ARM data, and Yang et al. (2011) used EMERALD1 data; however, these studies are only loosely based on observations and often the large-scale forcing of the cloud layer, which is so important for cloud development (see Lin et al. 2002) is either not available or very approximate.

Comparisons to observations have improved in recent years in that efforts have been made to simulate the remote sensing of radar and radiometers within the models for ease of comparison when evaluating timeseries (Marsham and Dobbie, 2005; Marsham et al., 2006), as well as making use of more and more observations such as modelling returns of Doppler fall velocities (Marsham et al., 2006). Important advances have been made by observationalists since the last inter-comparison in using a synergy of more than one instrument to improve retrievals (Deng and Mace, 2006; Delanoe and Hogan, 2008). In this work we utilise remote sensing to determine ice content, ice number and fall velocities. This offers great opportunities to test models since models can be easily tuned to a single observation of, say, ice water content (IWC) or ice number concentration (INC); however, observations of three or more variables affords a much better opportunity to highlight models performing well and also highlight potential deficiencies. We note that one case study is not a definitive assessment of the cirrus models, but offers a good basis to begin with and build upon.

It is important for the cirrus research community to assess current cirrus models and schemes against rigorous observations to determine if cirrus modelling has improved from the

developments over the last decade and also use the results to gauge which models are performing well and identify areas for improvement. This is the first cirrus study that includes rigorous comparisons to observations with the added benefit of an inter-comparison framework. This paper begins with describing the observed case of 9 March 2000 at the ARM SGP site and then proceeds to detail how the modelling case was established. This case was issued to the GCSS cirrus working group members to participate in the modelling inter-comparison; the results of which will be presented in a follow-on paper.

2 ARM SGP IOP 9 March 2000 observations used in the case development

The main aim of the current GCSS cirrus inter-comparison was to compare the model results to observations in order to evaluate model performance. As mentioned, the last inter-comparison showed strong model-to-model variation for results such as IWP with time for even such an idealised case. It is imperative that the cirrus community evaluate their models with observations in as rigorous a way as possible and through multiple comparisons. This case, presented in this work, forms the first step in that process.

The 9 March 2000 case was selected because it was a well-observed case. During the intensive observing period (IOP) at the SGP ARM site in March 2000, cirrus formed just upwind from the site on the 9th and advected directly over the Central Facility (CF) site. The ARM sites have the most extensive set of routine measurements in the world and this is enhanced with aircraft and supplemental measurements during IOP periods. In addition to the extensive observations taking place, analysis of some key results from the 9th were readily available for the inter-comparison. This included remote-sensing retrieval of cloud properties, analysis of aircraft observations and objective analysis (Zhang et al., 2000). Unfortunately, aerosol properties were not available at the cloud layer altitude during the cloud evolution relevant for our case development.

2.1 Meteorology and profiles

The region of cirrus that eventually was observed at the CF was first noted as a jet stream maximum in a southwesterly flow that passed over the mountain ranges of central New Mexico. The cirrus thickened as the disturbance approached central Oklahoma and the cloud features appeared to organise into longitudinal bands. Satellite imagery suggested active development of individual features within these bands as the system passed over the CF. The character of the cirrus in the satellite plots as well as the large scale atmospheric flow suggests that the cloud may be forced by gravity waves from the neighbouring mountains. The objective analysis predicted a weak lifting, whereas the RUC model indicated little to no ascent. This is explored further in the large scale forcing section below.

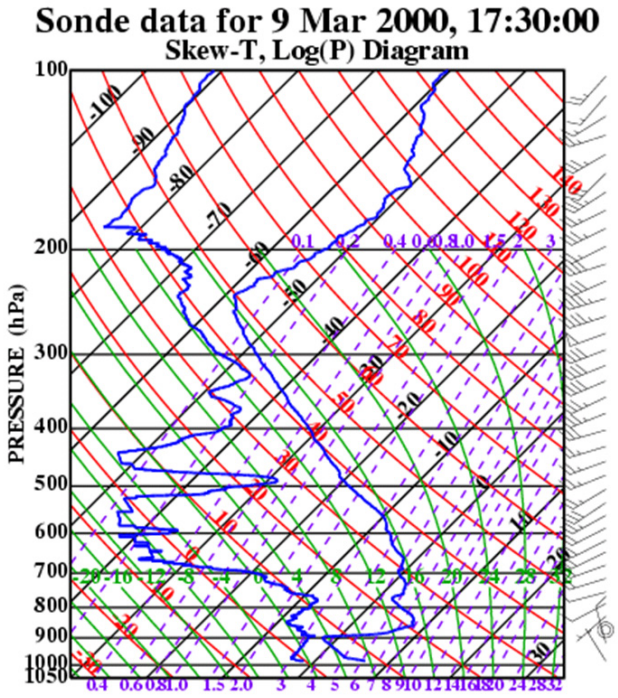

Fig. 2. Tephi-graph for the 9 March 2000 case study. The meteorological soundings are taken from radiosonde ascents and indicate the high water vapour between 300 mb and 350 mb level where the cloud forms.

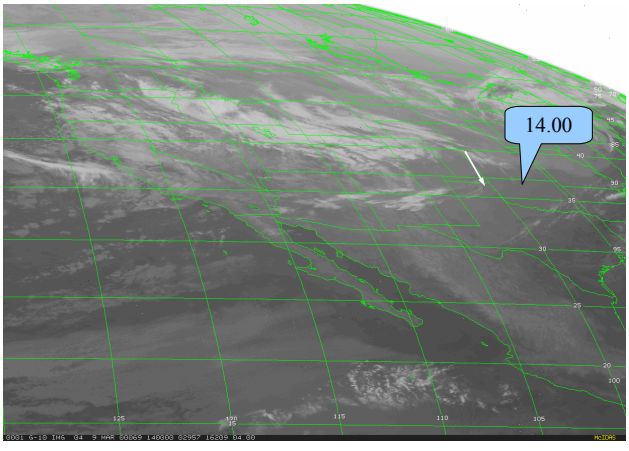

Fig. 3. GOES10 satellite plot at 14:00 UTC on the 9th of March 2000. The white arrow indicates approximately where the cirrus forms upwind and the ARM Central Facility is denoted by the blue indicator.

The radiosondes were released simultaneously at five locations at three hour intervals during 9 March, including the CF site and four sites surrounding the CF. These were used to construct the profiles, such as temperature, pressure,

horizontal wind profiles used in the case. The profiles indicated a temperature inversion near cloud top and a water vapour peak at 8–9 km, where the cloud is observed, as shown in Fig. 2.

2.2 Remote sensing

Visible satellite images were analysed from both GOES 8 and 10 for the time period from 00:30 UTC to 23:30 UTC on 9 March 2000. In Fig. 3, the blue indicator (with the time of 14:00 UTC inside) points to the ARM SGP CF site and the white arrow indicates the location where the cirrus cloud system was first observed to form upwind and south west of the CF. The cloud system is observed to brighten and become more extensive in subsequent visible imagery as it advects from the location of formation to the ARM SGP site. The cloud is observed by the MMCR at the CF approximately 210 min (at 17:30 UTC) after the time of formation.

The remote sensing of the cirrus cloud properties such as IWC, INC, and ice particle fall speeds is crucial to the case study. An important reason for choosing this case study was that these cloud properties were already analysed (by G. G. Mace, Utah) and available for this study (Mace, 1998). The retrieval is based on algorithms using radar reflectivity and downwelling infrared radiances to evaluate the cirrus cloud microphysical properties (Matrosov et al., 1992; Matrosov et al., 1994). The layer-averaged properties of optically thin cirrus is applied, which is calculated by using the observational platforms at the ARM sites. The layer-mean particle size distribution (PSD) (Mace, 1998) is the main assumption in this method, in which a modified gamma function (Dowling and Radke, 1990) is used. The PSD equation is

$$N(D) = N_{\mathrm{x}} \exp(\alpha) \left(\frac{D}{D_{\mathrm{x}}}\right) \exp\left(-\frac{D\alpha}{D_{\mathrm{x}}}\right) \quad (1)$$

where D_{x} is the modal diameter, N_{x} is the number of particles per unit volume, per unit length at the functional maximum and α is the order of the distribution, which is suggested ≤ 2 for cirrus (Dowling and Radke, 1990).

Shown in Fig. 4 is the retrieved IWC, INC, effective size and mean mass length, etc., as functions of time. The errors in IWC and median particle size are of the order of 60 % and 40 %, respectively (see Mace et al., 2002). The case development focuses on cloud that first forms upwind and then advects over the SGP CF site and is remotely sensed at 17:30 UTC (shown in Fig. 4). It is evident in the retrievals that the cloud increases in IWC as it advects over the SGP site and thickens in vertical extent.

2.3 Aircraft turbulence observations

University of North Dakota's Cessna Citation aircraft undertook 12 flights as part of the IOP, in March 2000, including flight penetrations at various altitudes through the cirrus cloud on the 9th. This flight started at 18:32 h which is after our first cloud appearance at the CF, so it is not an exact match with our comparison time. But it appears reasonable to assume that the turbulence observed by the aircraft measurements is representative for the cloud at an earlier stage. The mean wind and wind turbulence were measured by five-hole-probe (Validyne P40d) in combination with INS/GPS (Litton LTN-76). The sampling rate is 25 Hz and the uncertainty for turbulent fluctuations is about $0.05\,\mathrm{m\,s^{-1}}$. The true airspeed (to estimate length scales) was mostly about $120\,\mathrm{m\,s^{-1}}$. The power spectra of the vertical wind velocity, w, along flight legs at different altitudes, as shown in Fig. 5, indicates a scale separation at about 320 m length scale (roughly 0.4 Hz). The scale of large eddies is about 200 m (roughly 0.6 Hz) and the inertial sub-range starts showing up at a scale of about 100 m (roughly 1.2 Hz). The power spectra indicates that the turbulent kinetic energy is considerably higher in the cloud top region compared to the base. Based on the scale lengths deduced from the turbulence observations, we decided that 100 m grid resolution in the cloud layer for the LEM simulations would be appropriate.

2.4 Large scale forcing

The large scale forcing is critical for obtaining a good modelling case study, as it has such an important influence on the formation and magnitude of the cloud. For the March 2000 IOP at the ARM SGP site, objective analysis has been performed to assess the large-scale forcing, so we begin with this.

2.4.1 Objective analysis

Objective analysis for the March 2000 IOP and results are summarised in Zhang et al. (2000). We summarise key points from the paper below; for specific details of the method please refer to Zhang et al. (2000). The objective analysis used is a constrained variational analysis method (CVAM) which was originally developed by Zhang and Lin (1997) with a second improvement in 2000. CVAM was developed for deriving large-scale vertical velocity and advective tendencies from sounding measurements and works with the raw data from even a small number of stations. It can refine these atmospheric state variables as well as give uncertainties in the original data. The CVAM approach requires large-scale variables (u, v, T, q), surface measurements including surface sensible and latent heat fluxes, precip, surface pressure, surface winds, surface temperature, surface broadband net radiative flux and column total cloud water.

The observed data for these variables are used in this analysis which includes conservation of column-integrated mass, water, energy and momentum (Zhang et al., 2000). The data used in the CVAM approach are variables collected from the ARM balloon-borne sounding and National Oceanic and Atmospheric Administration (NOAA) wind

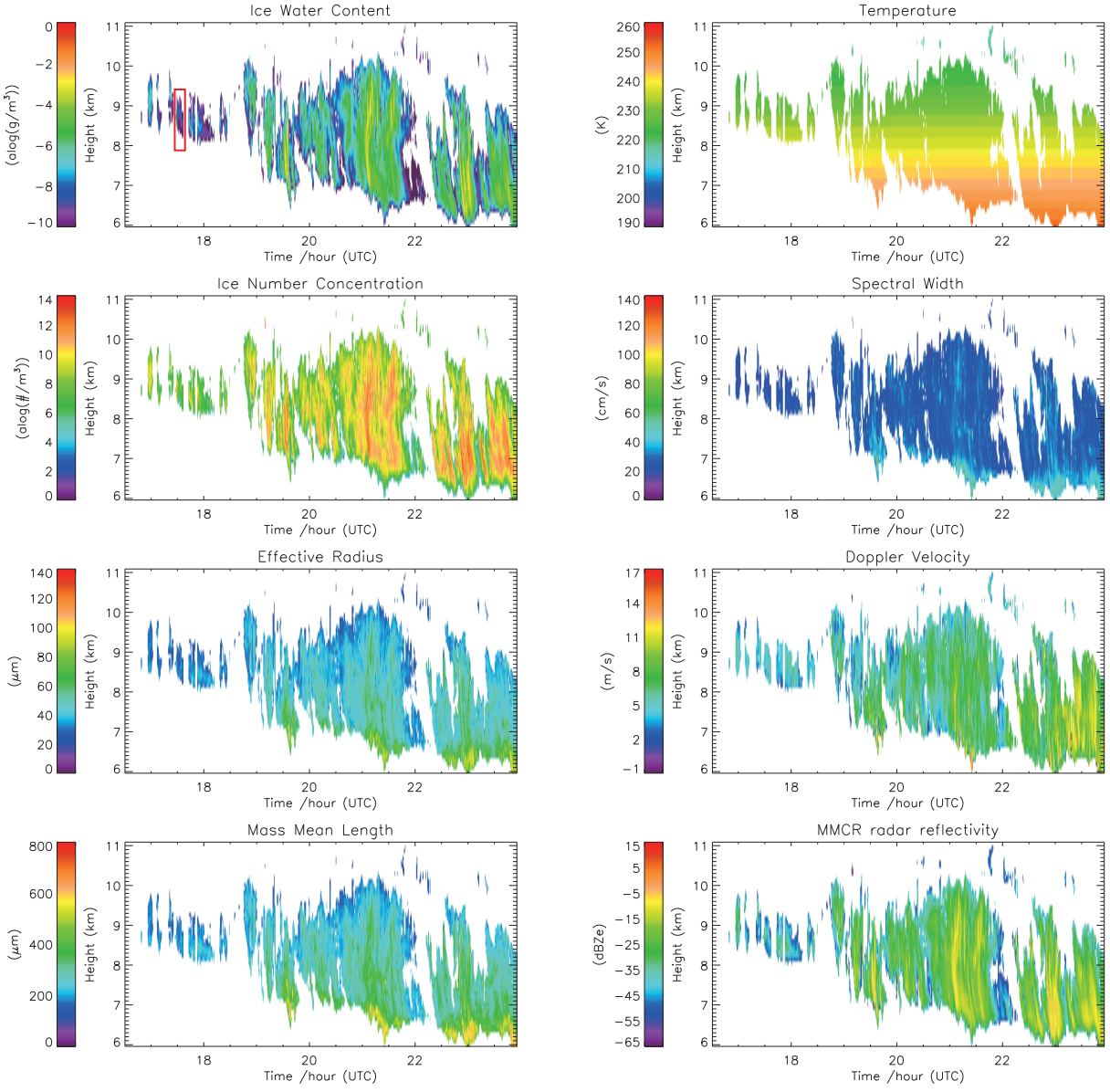

Fig. 4. Remotely sensed quantities as a function of height and time. The quantities include total IWC, total INC, effective radius, mean mass length, temperature, spectral width, Doppler velocity and reflectivity. Units indicated in the plots. The plots based on retrievals at the ARM SGP CF for 9 March 2000. The inter-comparison is based on the cloud when it arrives at the CF at approximately 17:30 UTC and indicated on the left side of each plot. The red box in the top left panel indicates the comparison period for modelling and retrievals.

profile measurements. Figure 6a shows there is one balloon launch site located at the CF of the ARM site and another four launch sites around the CF at the boundary facilities.

During the IOP 2000, sounding balloons were launched every three hours to measure the variables such as temperature, pressure, water vapour mixing ratio and wind profiles. In addition, the objective analysis makes use of seventeen NOAA wind profilers surrounding the SGP site. Seven of which are near the CF and five vertical profilers exactly overlap with the sounding stations, as shown in Fig. 6b. The seven sites constitute the domain of the objective analysis. One additional grid point is added in each boundary site to improve the linear assumption Fig. 6c. The Cressman scheme (Cressman, 1959) is used for the upper air measurement, making use of the general weighting function according to:

$$w_{ik} = w(x_i, x_k) = \begin{cases} \frac{1}{N} \frac{L^2 - (x_i - x_k)^2}{L^2 + (x_i - x_k)^2}, & d_{ik} < L \\ 0, & \text{otherwise} \end{cases} \quad (2)$$

where the w_{ik} is the weighting coefficient, k indicates the observational points and i is the analysis grid point, x_i is any variable in three or four dimensions at the grid point,

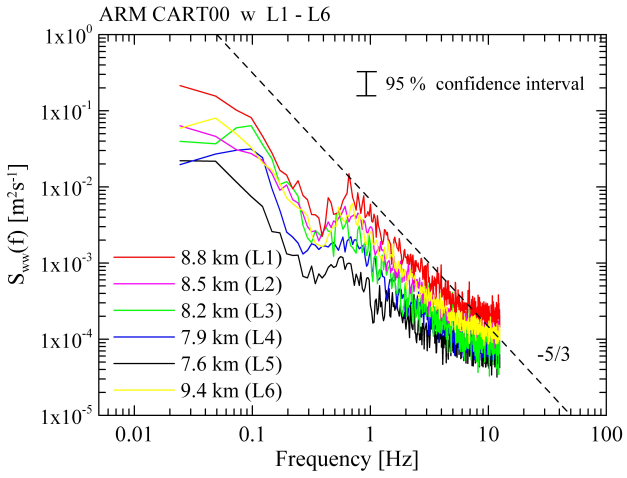

Fig. 5. Power spectrum of vertical velocity obtained from aircraft observations. Pertinent scales are: separation length scale is 320 m∼0.4 Hz, large eddies occur at roughly 200 m∼0.6 Hz, and the inertial sub-range starts showing up at a scale of about 100 m∼1.2 Hz.

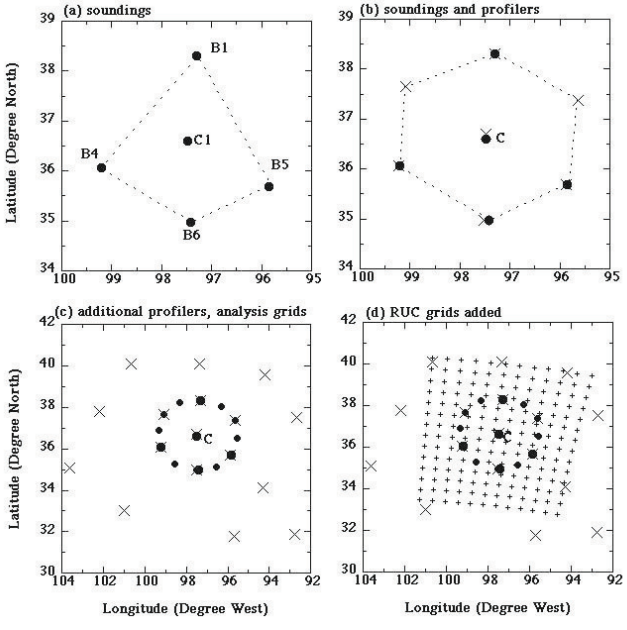

Fig. 6. Latitude and longitude locations of the **(a)** radiosonde launches, **(b)** the radiosonde launch sites and profiles, **(c)** additional profilers and grid, and **(d)** the RUC model grid. (The plots are taken from Zhang et al., 2000).

x_k ($k = 1, 2, ..., K$), observation stations, N_i is the number of measurements within distance L, and d_{ik} is the distance between the measurements and grid point.

The output from NOAA RUC is used in Eq. (3) as the value for the background function, f_b (shown in Fig. 6d). The

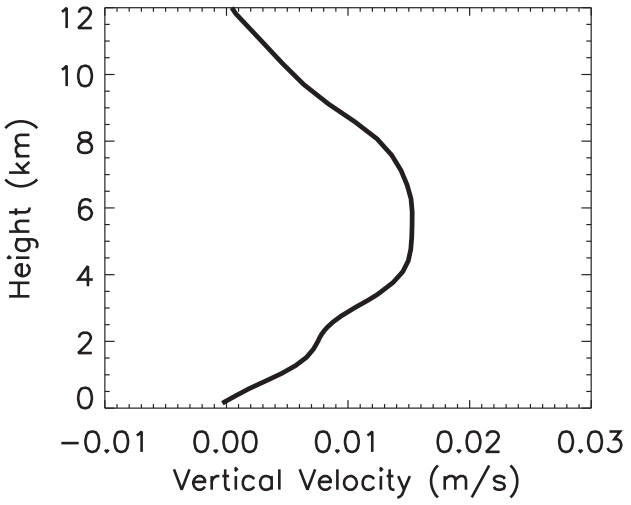

Fig. 7. Large scale vertical velocity from OA at 03:00 pm 9 March 2000.

general form used to evaluate the objective analysis variables at each grid-point is given by:

$$f_a(x_i) = f_b(x_i) + \sum_{k=1}^{k=K} w_{ik}[f_o(x_k) - f_b(x_k)] \quad (3)$$

For further details refer to Zhang et al. (2000). There is also a comprehensive set of surface measurements, as indicated in Table 1, around the SGP site and measurements from satellites such as GOES.

There are three frequently used area-based data analysis approaches for objective analysis including the analytical fitting method, the line integral method and the regular grid method. The ARM SGP objective analysis method uses a hybrid approach of the regular-grid and line integral methods and a variational constraining procedure (Zhang and Lin, 1997). The large scale variables diagnosed from the objective analysis are listed in Table 2.

From the objective analysis, we illustrate in Fig. 7 the large scale vertical motion at 15:00 UTC which is at the time the cirrus has already formed and is advecting toward the CF at SGP. The vertical velocity at 8–9 km height is approximately 0.01 m s^{-1}.

2.4.2 RUC model results

To complement the OA, we also investigated the large scale forcing predicted by the RUC model. The regional (large-scale for our 10 km domain high resolution simulations) scale updraft is obtained using the profiles from the objective analysis with the RUC operational atmospheric prediction system. RUC is an analysis system and numerical forecast model which had its origins in the Mesoscale Analyses

Table 1. The surface measurement used by the objective analysis at the ARM SGP site at Oklahoma USA, used for the objective analysis during the 9 March 2000 campaign and the variables measured by each instrument.

Platform Name	Variables Measured
Surface Meteorological Observation Stations(SMOS)	surface pressure, surface winds, temperature, humidity
Energy Budget Bowen Ratio (EBBR) Stations	surface latent and sensible heat fluxes, surface broadband net radiative flux
Eddy Correlation Flux Measurement System (ECOR)	surface vertical fluxes of momentum, sensible heat flux, latent heat flux
Oklahoma and Kansas mesonet stations (OKM and KAM)	surface precipitation, pressure, winds, temperature
Microwave Radiometer (MWR) stations	column precipitable water, total cloud liquid water
GOES satellite	clouds and broadband radiative fluxes

Table 2. The diagnosed variables output by the Objective Analysis

Relative Humidity	Surface Temperature
Dew Point	Sea-level pressure
Precipitation	Snow accumulation
snow depth	Precipitation type
Freezing levels	3 h pressure changes
CAPE/CIN	Lifted Index
Precipitable water	Helicity
Soil moisture	Tropopause pressure
Vertical velocity	PBL depth
Gust wind speed	Cloud base height
Cloud fraction	Visibility
Pressure of max Theta-E in column	convective cloud top height
Equilibrium level height	

and Prediction System (MAPS) which was developed at the Forecast Systems Laboratory (FSL) in 1988. The first RUC model with a 3 h data assimilation cycle, 60 km resolution, and vertical 25 levels was established at the National Center for Environmental prediction (NCEP) in 1994. In 1998, this was followed by the RUC-2 model which had a 1 h data assimilation cycle, 40 km resolution and 40 levels. RUC-20 (20 km resolution, 50 levels) and RUC13 (13 km resolution, 50 levels) were developed in 2002 and 2005 separately. Providing short range weather forecasts is the primary use of RUC model and evaluation of other models. The diagnostic variables derived from RUC model is listed in Table 2.

The RUC model, being initialised with updated data every hour, is a great strength as well as the fact that all the data are on isentropic vertical levels. The horizontal resolution, however, is a weakness for this case as it is still insufficient to describe local topographical circulations for this high resolution case.

For 9 March, the RUC model indicates little to no ascent rate (approximately zero and certainly bounded by $0.0016\,\mathrm{m\,s^{-1}}$) in the region in which the cirrus cloud is formed. So in summary, the objective analysis indicates a weak ascent whereas the RUC model indicates essentially no ascent. Since the objective analysis is making use of observed local data to where the cloud is observed and this data may contain signatures in the data of local forcings, we seek to explain the difference in forcings between the objective analysis results and the RUC model prediction.

Given that the direction of the mean atmospheric flow at cloud level is over the Rocky Mountains on the 9 March and the SGP CF is on the lee side of the mountains, the vertical motion could be explained by gravity waves. This could explain why the objective analysis suggested a larger vertical velocity than the RUC model. In order to evaluate the potential of gravity waves to influence the cirrus formation, we have performed gravity wave simulations for the whole of the USA for 9 March 2000 using the model 3DVOM described in the next section.

2.4.3 Gravity wave analysis using 3DVOM

As shown in Fig. 8, the most prominent topological feature in this map of the USA is the Rocky Mountains (RM). The RM extend for more than 3000 miles in length and cover approximately 300 000 square miles and are positioned to the west of the SGP ARM site. With a south-west atmospheric advection, the influence of gravity waves on the cirrus formation on the lee side of the mountains is highly likely.

In this study, we make use of the 3DVOM model called 3-D velocities over mountains which is a finite-difference numerical model designed for high-resolution simulations of lee waves generated by flow over complex terrain.

The model is based on a set of time-dependent, simplified, quasi-linear equations of motion for a dry atmosphere (see Vosper and Worthington 2002; 2003 for details), typically run with European Centre for Medium Range Weather Forecasting (ECMWF) winds. The model was run at a 1 km resolution for the entire USA, initialised in this case with NCEP winds and the topology specified from the data that went into making Fig. 8.

The resulting map of gravity wave vertical motion determined by 3DVOM at the cloud level is shown in Fig. 9. It shows clearly that gravity waves are predicted to cause ascending motion in the region where the cloud forms (roughly 300 km upwind) and during much of its advection toward the SGP CF site. Consequently, to obtain the vertical forcing for the high resolution cloud resolving simulation, we extracted

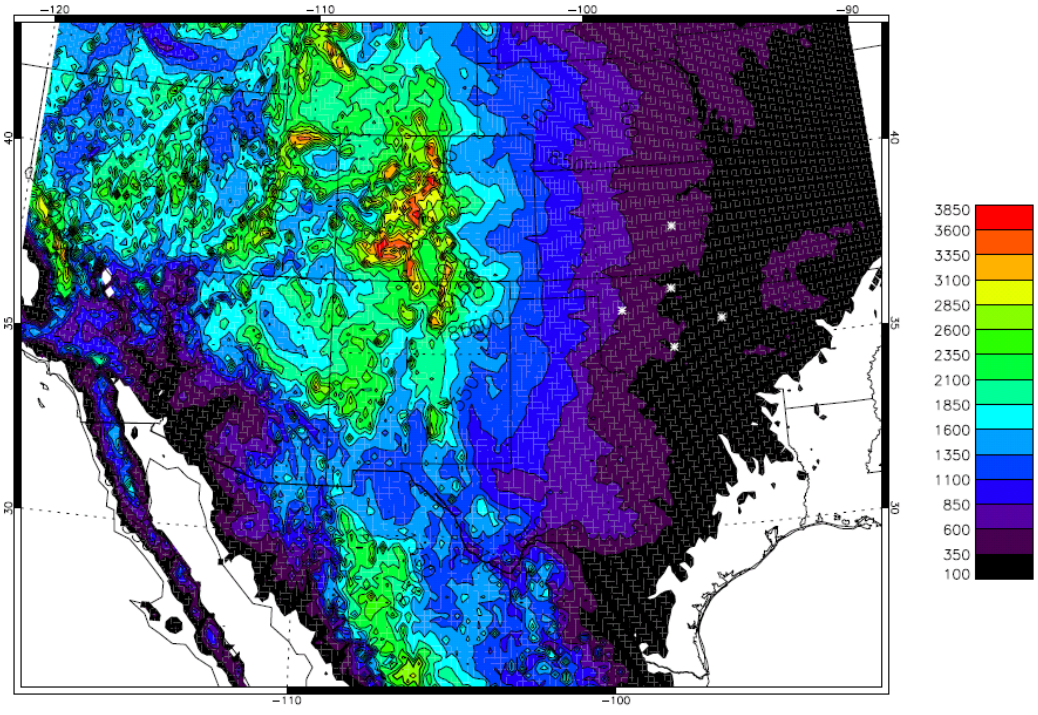

Fig. 8. Topology of the USA (m). This is used to initialise the surface heights for the gravity wave simulations in the 3DVOM model. The white dots indicate the ARM SGP Central and Boundary Facilities (data from Global Land One-km Base Elevation (GLOBE) project).

the vertical forcing from Fig. 9 along the advection path of the cirrus cloud from formation to the SGP CF. The gravity wave forcing at cirrus cloud level as a function of time is given in Fig. 10.

The plot of vertical velocity forcing as a function of height and time, shown in Fig. 10, indicates gravity waves superimposed with various wavelengths that are undergoing an ascent (hence cooling) beginning at the location where the cirrus is observed to first form. This agrees very well with where the cloud forms from satellite observation and the gravity wave forcing intensifies as the cloud advects toward the SGP site, in agreement with the satellite observation. In the final stages of when the cloud is advecting over the SGP site, the gravity wave undergoes descent. So the modelled gravity wave forcing provides ascent or cooling to the cloud layer that is consistent with maintaining a cirrus cloud layer as it advects toward the CF site. We also note that the mean vertical velocity from the gravity wave simulation agrees well with the vertical velocity from the objective analysis.

3 Model setup and first results

We now describe how the observations were used to set up the modelling study and first results are illustrated just for the UK Met Office large eddy simulation model (LEM) to test if the case is appropriate for an inter-comparison. We begin with a brief description of the LEM model.

3.1 UK LEM Model

To establish the modelling case based on the 9 March ARM SGP observations, we used the UK Met Office Large Eddy Model (LEM) v2.3 (Mace, 1998; Gray et al., 2001). The UK Met Office LEM performs numerical integrations using basic equations for momentum, thermodynamics and continuity. The model is non-hydrostatic and uses the deep anelastic approximation (quasi-Boussinesq) which allows for small pressure and density variations from the reference hydrostatic state. Periodic boundary conditions are used at the horizontal edges of the domain and rigid lid conditions are used at the surface and top of model boundaries. The model has been used for several studies of cirrus (Dobbie and Jonas, 2001; Marsham and Dobbie, 2005; Marsham et al., 2006; Yang et al., 2011). The version we use has a fully integrated Fu-Liou radiation scheme to address the radiative properties and heating rates of the cloud. Details of the radiation scheme are provided below and in papers such as Dobbie and Jonas (2001), Marsham and Dobbie (2005) and Marsham et al. (2006). We provide a brief description here. The radiation model used is based on Fu and Liou (1992, 1993) with an ice radiation package (Fu, 1996; Fu et al., 1998) and is coupled with the LEM and used to assess cirrus radiative properties, as

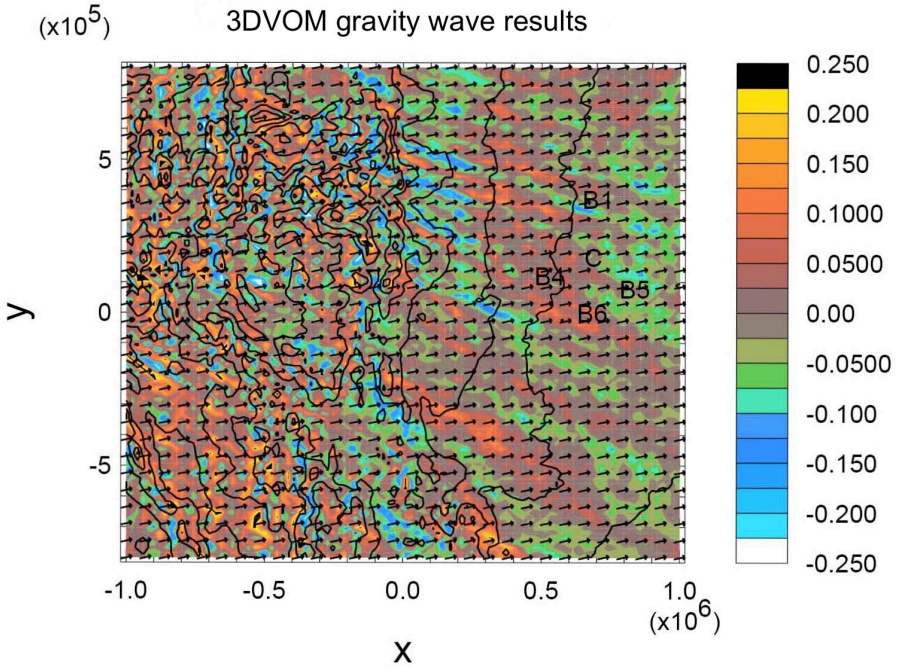

Fig. 9. Gravity wave plot at the cirrus level for 9 March 2000. Colour codes indicate ascent rate (positive) or descent (negative) in $\mathrm{m\,s^{-1}}$. These results are derived from the output of 3DVOM model runs.

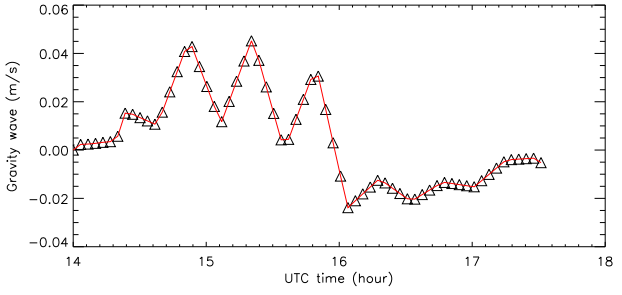

Fig. 10. Modelled gravity wave forcing ($\mathrm{m\,s^{-1}}$) versus time (h). This is the modelled gravity wave forcing that the cloud experiences as it advects from where it first formed to when it arrives at the ARM SGP CF, where it is observed by the MMCR radar.

was done by Dobbie and Jonas (2001), Marsham and Dobbie (2005), Marsham et al. (2006) and Yang et al. (2011). The radiative transfer equation solution is derived using the discrete ordinates delta four-stream solution approach as discussed in Liou (1986) or papers such as Li and Dobbie (1997).

The Fu-Liou δ-four-stream model is a 1-D algorithm that is applied to all columns independently. The Fu-Liou radiation model has six solar and twelve infrared bands. The scheme is linked to the water in the LEM including ice, liquid droplets, rain, graupel, snow and water vapour. For the case study, the optical properties are specified using the cloud IWC and a value of generalised effective size of 35 µm (a similar approach also used in water clouds, see Dobbie et al., 1999), which is in keeping with the observations after converting between generalised effective size and effective size and observations more generally (see Fu, 1996). Rayleigh scattering is treated for molecules and gaseous absorption is implemented using a correlated k-distribution method including gaseous absorption by O_3, CO_2, CH_4, N_2O and H_2O. The CO_2, CH_4 and N_2O are assumed to have uniform mixing ratios throughout the atmosphere with concentrations of 330, 1.6 and 0.28 ppmv, respectively.

3.2 Model setup for the GCSS inter-comparison

The model domain size was 10 km in the horizontal by 20 km in the vertical. The horizontal resolution was set to 100 m and a variable vertical resolution was used with 100 m resolution for much of the domain (from 5 km to 10 km) and including the cloud layer, with lower resolution above and below this region. The resolution was selected based on the aircraft turbulence analysis presented which indicated it was an appropriate scale in which to separate resolved and unresolved motions. The model simulation time was four hours duration. Time zero is associated with 14:00 UTC when the cloud first forms. No cloud is initially specified in the model.

At the first time step of the simulation, random perturbations in potential temperature of $\pm 10\,\%$ and water vapour mixing ratio of $\pm\,5\,\%$ are imposed between 6 and 10.5 km to

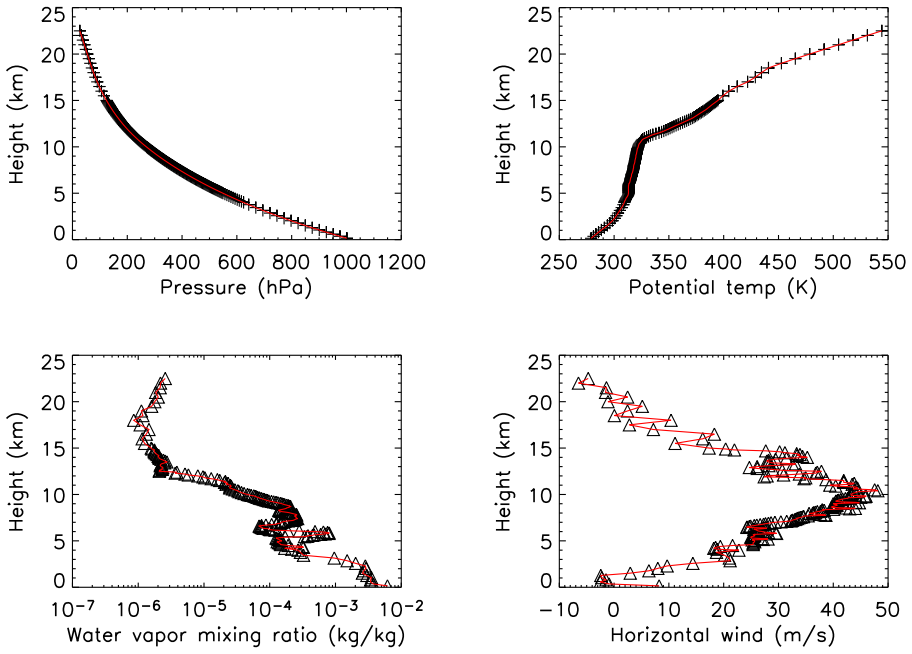

Fig. 11. Initial profiles of pressure, potential temperature, horizontal wind and water vapour mixing ratio at the start location upwind from the CF. The profiles are obtained by taking the observed values at the CF and backtracking them through the effects of the gravity wave to the starting location. This ensures that the profiles will be as observed after the effects of the gravity wave in the modelling.

establish initial inhomogeneity in the cloud layer (see Marsham and Dobbie, 2005).

We impose two forcings on the simulations in the intercomparison, first a large scale gravity wave forcing updated every 201 s during the simulation. The gravity wave forcing is applied throughout the whole vertical domain for simplicity. Second, a Solar and infrared radiative heating profile is applied at every time step and updated every 5 min.

Periodic boundary conditions are used at the horizontal limits of the domain and in the vertical no slip conditions are imposed at the surface and top of the model atmosphere. Heterogeneous and homogeneous nucleation modes are permitted in the runs. Horizontal winds are specified from the radiosonde vector-resolved winds into the direction of the advection.

The MMCR based at the SGP CF is the key remote-sensing tool used to obtain the comparison fields for the case and so its location at CF is the point at which the cirrus cloud is compared quantitatively with the remote sensing. The cloud, however, forms approximately 300 km upwind from the CF. Thus, we have a choice to either spin-up the modelled cloud to agree with the observations at the CF (thereby ignoring the formation and evolution phase) or to model the formation and evolution during advection to the SGP CF and compare with observations at that time.

For this case development, the latter approach was taken, to form the cloud in the model based purely on the forcings acting to create the cloud rather than spin up the model cloud to artificially "agree" with an observed cloud which has a long history of evolution and is continuously changing as it advects over the observing point at the SGP CF.

So we must recreate the conditions upwind when the cloud formed. We have a few constraints available to do this. From the satellite observations, the cirrus cloud was observed to first form at 14:00 UTC and took about 210 min to advect to the CF, roughly 300 km distance. Also, we know the thermodynamic profiles observed at the CF after the cloud advects to the CF. This is after the profiles have undergone forcings during the prior 210 min during the time when the cloud advects from formation location to the CF. Therefore, to obtain the profiles local to where the cloud formed, we apply the forcing in reverse to obtain the initial profiles. This ensures that when the profiles are forced during the 210 min advecting to the CF they will then agree with the observed profiles.

We know the cloud first forms with the initial upwind profiles. It was necessary to adjust the initial cloud layer relative humidity to have a slight super-saturation with respect to ice of 10 %. This was equivalent to applying a small temperature adjustment of 1–2 K in the cloud layer, which is within observed error, so as to ensure that cloud formation occurred immediately (as observed) when modelled. With this small adjustment, the cloud forms at the observed time. We have performed runs for initial vapour profiles both with and without the Miloshevich et al. (2001) correction applied to the water vapour profile (see Figs. 13 and 14). We note that with the corrected profile, we again adjust to a slight

super-saturation with respect to ice of 10 % at the time of when the cloud is observed to begin to form. The initial profiles are shown in Fig. 11. To ensure that the small adjustment did not dictate the cloud IWC when compared to observations at 210 min, runs were performed without the gravity wave forcing applied (only the small initial super-saturation remained). The cloud initially formed a low IWC cloud that dissipated quickly. Therefore, the small adjustment ensured that the cloud formed at the observed time and that the cloud IWC of the simulation was dictated by the gravity wave forcings and not due to uncertainty in the initial profile.

The above modelling case ensures that the cloud forms at the correct time and evolves under the influence of the external gravity wave forcing and can be compared to observations at the CF after the 210 min duration of model run. For the initial comparison, we used a 2-D simulation and performed the run for a four hour duration and compared with observations at 210 min. The 2-D domain is not for the full 300 km domain which is more computationally taxing for high resolution simulations, not to mention problematic for periodic boundary conditions and a spatially varying forcing. The horizontal domain is 10 km which is taken to be a local region of cloud. The domain should be viewed as a Lagrangian domain advecting (and so advective tendencies which are small are ignored) with the mean wind from the cloud formation site to the CF site. The initial profiles of wind have their shape retained so as to ensure the correct shear is used in the simulation, which is essential. The cirrus layer is completely detached from surface and boundary layer influences and so the mean wind-field is not important. First results are shown for LEM 2-D simulations described in the next section. The case data files are available at: http://homepages.see.leeds.ac.uk/~lecsjed/huiyi/gcss/.

3.3 First model comparisons to the GCSS case study

The UK Met Office LEM model version 2.3 was used to do a first test simulation of the case to evaluate the performance of a representative high resolution cloud model in preparation for the inter-comparison. Figure 12 shows the results of the LEM simulation at four times: 60, 120, 180 and 210 min. The time of 210 min is when the cirrus cloud is to be compared to observations. The growth and then decay of the ice water mixing ratio (IWMR) in Fig. 12 illustrates the importance of the gravity wave forcing on dictating the time evolution of the cirrus cloud.

In Fig. 13, we compare the cirrus IWMR to the retrieved results. The red crosses indicate the retrieved IWMR for a 10 min averaging period centred around 17:30 UTC. We see that the magnitude of the cloud modelled cloud IWMR (roughly 2×10^{-7}kg kg^{-1}) is in reasonable agreement to retrievals. No tuning of parameters was performed in the model run. We note that the cloud depth is similar in both the observed and modelled results. In Fig. 14, we compared the modelled and retrieved INC results. The red crosses are

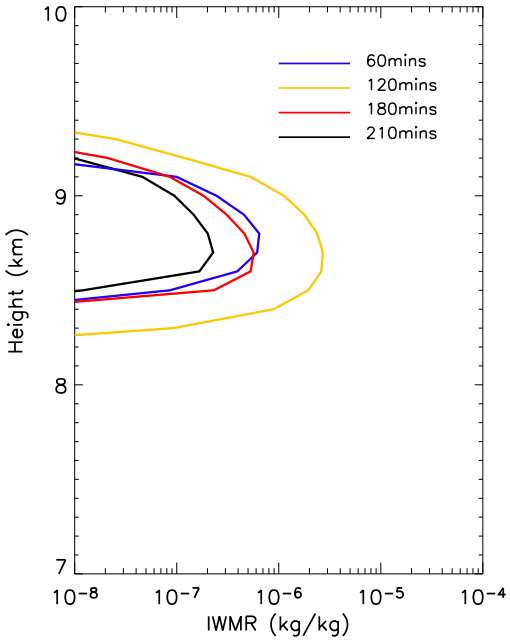

Fig. 12. Shown are the total ice water mass mixing ratio (kg kg^{-1}) (total indicates ice and snow which are ice aggregates in this simulation) versus height at four times during the UK Met Office LEM simulation: 60, 120, 180 and 210 min. The cirrus cloud modelled in the LEM is compared to observations at 210 min.

again the retrieved results. In the figure we note the cloud is of appreciable IWMR between the dashed lines indicating the cloud top and base from Fig. 13. This shows reasonable agreement of modelling to retrieved INC averaged over the same 10 min period. Based on the modelled and retrieved results for IWMR and INC the case appears appropriate for use in the model inter-comparison study. Model simulations compared to observations for fall speeds are presented in the follow-on GCSS inter-comparison paper. We now present radiative heating rates and then finish with discussing two important sensitivities for the case.

The radiative heating profile for both solar and infrared (IR) was also output by the LEM model and stored as a forcing to be used by the other models in the inter-comparison. The radiative heating by Solar and IR at the times of 60, 120, 180 and 210 min are shown in Fig. 15. The radiative forcing profiles were prepared for the inter-comparison at intervals of 5 min, which is deemed acceptable by assessing the rate of changes of cloud IWC.

We now discuss a couple of key sensitivities for the case. Sensitivities of the runs to heterogeneous and homogeneous nucleation were investigated since the cloud temperature was about $-38\,^{\circ}$C and, hence, it was possible for heterogeneous and homogeneous nucleation to play a role. We allowed both nucleation modes to be switched on in the

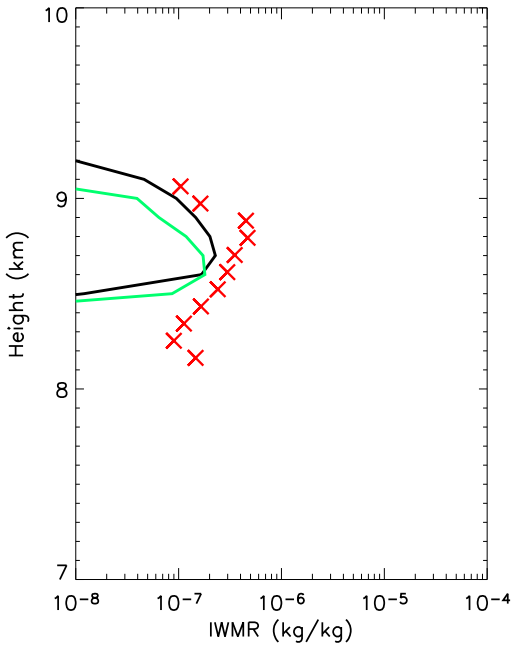

Fig. 13. IWMR ($\mathrm{kg\,kg^{-1}}$) versus height (km). The lines are modelled results and the red crosses are retrieved observations averaged over a 10 min period centred on 17:30 UTC. The black and green lines are indicated initial water vapour profiles corrected or uncorrected according to Miloshevich et al. (2001).

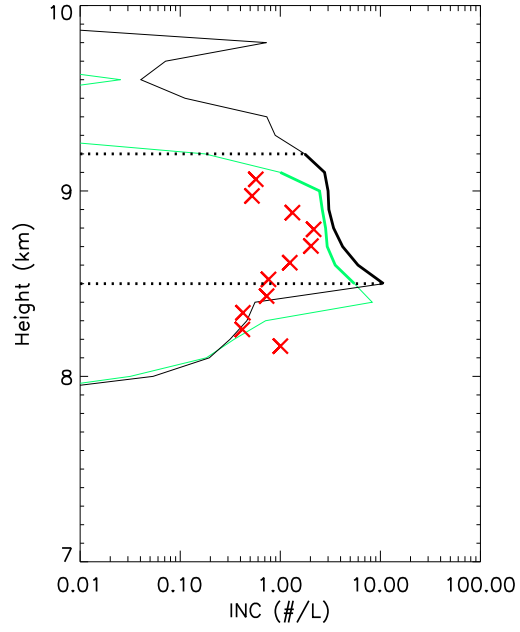

Fig. 14. Same as Fig. 13 except for INC. The two dashed black lines indicate the domain of significant IWMR corresponding to Fig. 13. The green and black lines are presented as thin in regions of negligible IWMR.

model runs. In the UK LEM model it uses the Meyers et al. (1992) scheme for heterogeneous nucleation. We have used the standard scheme and we have also run the model with a Meyers's nucleation capped at a maximum supercooling of −30 °C (see Vaughan et al., 2008), which for our modelled cloud showed very little difference compared to using the standard Meyers scheme (since supersaturations are often quenched before reaching this threshold). From the simulations and from the retrievals, we believe that heterogeneous nucleation is the dominant mechanism for the cirrus cloud in the early stages of the cloud (i.e., before 18:30 UTC). The observed average number concentration is approximately $1\,\mathrm{L^{-1}}$ (averaging in-cloud over a 10 min period centred on 17:30 UTC). Furthermore, the ascent rate predicted by the RUC model is below $1\,\mathrm{cm\,s^{-1}}$ and the objective analysis and gravity wave simulation predict up to a few $\mathrm{cm\,s^{-1}}$ ascent rate. Karcher and Lohmann (2003) illustrate the competition between heterogeneous and homogeneous nucleation for various updraft speeds and show that heterogeneous nucleation is dominant for updrafts up to about $6\,\mathrm{cm\,s^{-1}}$. Although the cooling promotes rising supersaturation, it rises slowly for slow updrafts and first leads to heterogeneous nucleation that produce ice particles that act to reduce the supersaturation through vapour deposition and prevent increasing supersaturation and reaching homogeneous nucleation. It depends also on the number of ice nuclei available which we do not have observations for, but we would not expect low concentrations in that region. Runs with only homogeneous nucleation switched on required much greater supersaturation driven by a stronger forcing, which did not agree with the strength of the forcings acting at the earlier stages of the cloud evolution (before 18:30 UTC). We agree with Solch and Karcher (2011) that homogeneous nucleation is likely to be dominant in the later stages of the cloud evolution when the cloud deepens dramatically after 18:30 UTC. This is consistent with the significant increases in cloud depth, the high IWCs and INC (up to $100\,\mathrm{L^{-1}}$).

The models involved in the GCSS inter-comparison range from 1-D through to 3-D and so it was important to assess the influence of model dimensionality for the case. To-date, there does not exist in the literature a testing of sensitivity of cirrus to model dimensionality for a wide range of forcings or specifically for the magnitude of forcing that is applied in this case. To illustrate the importance of dimensionality for our case, we present model results in Fig. 16 showing various combinations of ratios of 1-D and 2-D to 3-D results. The clouds are set up in the same manner as the standard case developed in this study except for the 1-D runs, where we used an ensemble of 30 1-D runs since the 1-D results are initialised with a single random perturbation in each vertical level. So different random perturbations were used for each run in the ensemble. The ensemble average of IWP was compared to 3-D model results.

It is shown in Fig. 16 that the 1-D to 3-D differ by as much as a factor of two (for appreciable IWP) early on in

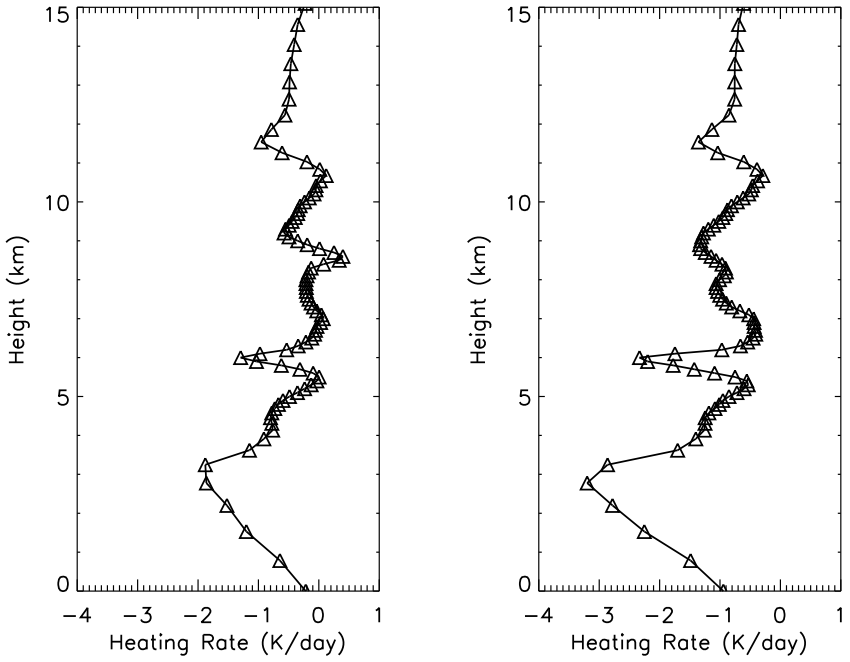

Fig. 15. Heating rate (K day^{-1}) profiles taken from the UK Met Office LEM model running with the Fu-Liou radiation scheme for 9 March 2000 at simulation times 120 and 210 min. The plots indicate very little variability in the heating rates except for about 8 to 9 km where the cloud forms and evolves.

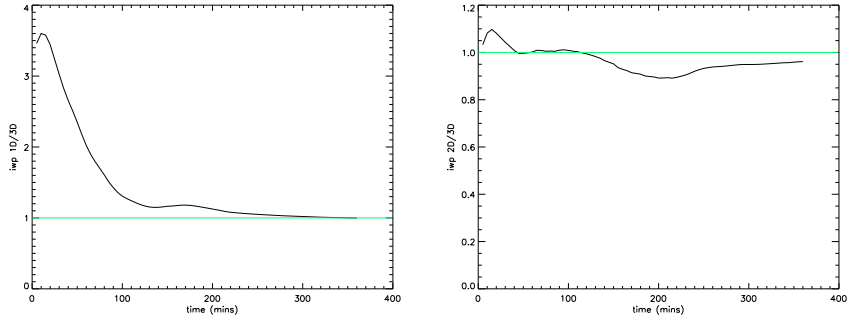

Fig. 16. The figure shows the modelled ratio of 1-D to 3-D IWP (left) and 2-D to 3-D IWP (right) as a function of time.

the simulation; however, at the comparison time of 210 min the difference is reduced significantly. The 2-D run compares well with the 3-D run for the full duration of the simulation so it illustrates that it is appropriate to use 2-D simulations for this case without significant differences to 3-D simulations for IWMR.

4 Summary

The previous GCSS cirrus inter-comparison (Starr et al., 2000) showed a wide range of results for idealised cases which raised concerns about the accuracy of cirrus modelling. Much was learned from that inter-comparison; however, there was no benefit of observations to help distinguish between model performances. Thus, a well-observed case study was decided as being the main focus of the current GCSS inter-comparison case study detailed in this paper.

The cirrus cloud observed at the SGP ARM site on 9 March 2000 was selected primarily because the cirrus cloud advected directly over the observing site during an enhanced observations campaign as part of the ARM SGP IOP for the month of March. The case makes use of valuable remotely retrieved values of IWC, INC and fall speed of ice particles. Having all three quantities is very beneficial for the inter-comparison in that it offers a far more discerning evaluation of models than comparing against a single quantity such as IWC.

The cirrus formed upwind from the SGP site and so we made use of GOES satellite remote sensing to determine the approximate time of cloud formation. The forcing that the cloud experienced during advection to the SGP site has been assessed using the RUC model, objective analysis and 3DVOM gravity wave simulations. We find that the forcings predicted by the objective analysis and gravity wave simulations are consistent in average magnitude and that the modelled gravity wave forcing correctly predicts the time and location of ascent where the cloud is observed to form. Initial testing of the case was performed with a cloud model to determine if the model would produce reasonably sensible results and thereby suggest that the case would be appropriate for a more detailed model inter-comparison study.

Modelling results were obtained using the UK Met Office LEM in 2-D mode. The resolution of the model runs was established by analysis of the aircraft turbulence observations, which indicated that the inertial subrange was at approximately 100 m. The model runs were developed as a quasi-Lagrangian 10 km domain moving with the mean advective velocity for the cloud layer. Results from the simulations indicate that the cloud IWC, INC and cloud thickness are in reasonable agreement. The cirrus cloud forms at the correct time, within observational uncertainty, under the forcing of gravity waves that were derived following the advection of the cloud from formation to the SGP site, as determined by the 3DVOM gravity wave simulations. Some important sensitivities were tested such as the dominant nucleation mode which is believed to be heterogeneous nucleation. Heterogeneous nucleation is consistent with the thin appearance and relatively low INC when the cloud advects over the ARM site in the early stages as well as the weak large scale forcings that were predicted by the objective analysis and models (3DVOM and RUC). LEM runs with and without homogeneous nucleation showed negligible differences. In addition, the model dimensionality was tested given that the inter-comparison will involve models running in 1-D, 2-D and 3-D. It was found that the 2-D performed similar to 3-D results, whereas a factor of 2 change was noted in the IWMR early on in the cloud development in switching to 1-D.

This paper presented the development of the case for the current GCSS cirrus inter-comparison. The intention of this work was to provide a well characterised case study that can be used not only for the inter-comparison, but will remain available to cirrus modellers for the future so that model updates and development of new cirrus models can be tested within its framework. In a follow-on paper, we will illustrate the inter-comparison results. Although one detailed comparison case is not enough to comprehensively test of cirrus models, this well-characterised case is an important step forward in evaluating our current capability and shortcomings in cirrus modelling.

Appendix

Abbreviations	
3DVOM	3-dimensional Velocities Over Mountains
ARM	Atmospheric Radiation Measurement
CF	Central Facility
CPMCP	Cirrus Parcel Model Comparison Project
CSMs	Cloud Scale Models
CVAM	Constrained Variational Analysis Method
ECMWF	European Centre for Medium Range Weather Forecasting
FSL	Forecast Systems Laboratory
GCMs	General circulation Models
GCSS	GEWEX Cloud System Study
GEWEX	Global Energy and Water Cycle Experiment
ICMCP	Idealized Cirrus Model comparison Project
INC	Ice number Concentration
IOP	Intensive Observation Period
IR	Infrared
IWC	Ice Water Content
IWMR	Ice Water Mixing Ratio
IWP	Ice Water Path
LEM	Large Eddy simulation Model
MMCR	Millimeter Cloud Radar
NCEP	National Center for Environmental Prediction
NOAA	National Oceanic and Atmospheric Administration
PSD	Particle Size Distribution
RM	Rocky Mountains
RUC	Rapid Update Cycle
SCMs	Single Column Models
SGP	Southern Great Plains
WG2	Working Group 2

Acknowledgements. Thanks to the Atmospheric Radiation Measurement (ARM) programme for providing data. We acknowledge Jon Petch (UK Met Office) as first mentioning potential gravity wave influences for the case. Thanks to Matt Woodhouse (University of Leeds) for input in responding to the reviewers comments regarding aerosol loadings. HY would like to thank Damian Wilson (Met O) for helpful comments and the UK Met Office for PhD part-funding.

Edited by: K. Gierens

References

Benedetti, A. and Stephens, G. L.: Characterization of errors in cirrus simulations from a cloud resolving model for application in ice water content retrievals, Atmos. Res., 59–60, 393–417, 2001.

Brown, P. R. A. and Heymsfield, A. J.: The microphysical properties of tropical convective anvil clouds: A comparison of models and observations, Q. J. Roy. Meteor. Soc., 127, 1535–1550, 2001.

Cheng, W. Y. Y., Wu, T., and Cotton, W. R.: Large-eddy simulation of the 26 november 1991 fire ii cirrus case, J. Atmos. Sci., 58, 1017–1034, 2001.

Cressman, G. P.: an operational objective analysis scheme, Mon. Wea. Rev., 87, 367–374, 1959.

Delanoe, J. and Hogan, R. J.: A variational scheme for retrieving ice cloud properties from combined radar, lidar

and infrared radiometer, J. Geophys. Res., 113, D07204, doi:10.1029/2007JD009000, 2008.

Deng, M. and Mace, G. G.: Cirrus microphysical properties and air motion statistics using cloud radar doppler moments. part i: Algorithm description. J. Appl. Meteor. Climatol., 45, 1690–1709, 2006.

Dobbie, J. S., Li, J. N., and Chylek, P.: Two- and four-stream optical properties for water clouds and solarwavelengths, J. Geophys. Res., 104, 2067–2079, 1999.

Dobbie, S. and Jonas, P.: Radiative influences on the structure and lifetime of cirrus clouds, Q. J. Roy. Meteor. Soc., 127, 1–20, 2001.

Dowling, D. R. and Radke, L. F.: A summary of the physical properties of cirrus clouds, J. Appl. Meteorol., 29, 970–978, 1990.

Fu, Q.: An accurate parameterization of the solar radiative properties of cirrus clouds for climate models., J. Climate, V9, 2058–2082, 1996.

Fu, Q., Yang, P., and Sun, W. B.: An accurate parameterization of the infrared radiative properties of cirrus clouds for climate models, J. Climate, V11, 2223–2237, 1998.

Fu, Q. and Liou, K. N.: Parameterization of the radiative properties of cirrus clouds, J. Atmos. Sci., 50, 2008–2025, 1992.

Fu, Q. and Liou, K. N.: On the correlated k-distributionmethod for radiative transfer in non-homogeneous atmospheres, J. Atmos. Sci., 49, 2139–2156, 1993.

Gray, M. E. B., Petch, J., Derbyshire, S. H., Brown, A. R., Lock, A. P., Swann, H. A., and Brown, P. R. A.: Version 2.3 of the met office large eddy model: Part ii: Scientific documentation, http://appconv.metoffice.com/LEM/docs/Scientific.ps, 2001.

Karcher, B. and Lohmann, U.: A parameterization of cirrus cloud formation: Heterogeneous freezing, J. Geophys. Res., V108, D14, 4402, doi:10.1029/2002JD003220, 2003

Li, J. and Dobbie, J. S.: Four-stream isosector approximation for solar radiative transfer, J. Atmos. Sci., V55, 558–567, 1997.

Lin, R. F., Starr, D. O., Demott, P. J., Cotton, R., Sassen, K., Jensen, E., Kaercher, B., and Liu, X. H.: Cirrus parcel model comparison project. phase 1: The critical components to simulate cirrus initiation explicitly, J. Atmos. Sci., 59, 2035–2329, 2002.

Liou, K. N.: Influence of cirrus clouds on weather and climate processes: a global perspective, Mon. Wea. Rev., 114, 1167–1199, 1986.

Mace, G. G.: Cirrus layer microphysical properties derived from surfacebased millimeter radar and infrared interferometer data, J. Geophys. Res., 103, 23207–23216, 1998.

Mace, G. G., Heymsfield, A. J., and Poellot, M. R.: On retrieving the microphysical properties of cirrus clouds using the moments of the millimeter-wavelength Doppler spectrum, J. Geophys. Res., 107, doi:10.1029/2001JD001308, 2002.

Marsham, J. and Dobbie, S.: The effects of wind shear on cirrus: A largeeddy model and radar case-study, Q. J. Roy. Meteor. Soc., 131, 2937–2955, 2005.

Marsham, J., Dobbie, S., and Hogan, R.: Evaluation of a large-eddy model simulation of a mixed-phase altocumulus cloud using microwave radiometer, lidar and doppler radar data, Q. J. Roy. Meteor. Soc., 132, 1693–1715, 2006.

Matrosov, S. Y., Orr, B. W., Kropfli, R. A., and Snider, J. B.: Retrieval of vertical profiles of cirrus cloud microphysical parameters from doppler radar and infrared radiometer measurements, J. Appl. Meteorol., 33, 617–626, 1994.

Matrosov, S. Y., Uttal, T., Snider, J. B., and Kropfli, R. A.: Estimation of ice cloud parameters from ground-based infrared radiometer and radar measurements, J. Geophys. Res., 97, 11567–11574, 1992.

Meyers, M., Demott, P., and Cotton, W.: New primary ice-nucleation parameterizations in an explicit cloud model, J. Appl. Meteorol., 31, 708–721,1992.

Philips V. T. J., Demott P. J., and Andronache C.: an empirical parameterization of heterogeneous ice nucleation for multiple chemical species of aerosol, J. Atmos. Sci., V 65, 2757–2783, 2008.

Randall, D., Curry, J., Duynkerke, P., Miller, M., Moncrieff, M., Ryan, B., Starr, D., and Rossow, W.: The second gewex cloud system study science and implementation plan, IGPO Publication Series, 34, http://www.ral.ucar.edu/projects/GCSS/WG5/GCSS_stuff/GCSS_2K.pdf, 2000.

Solch, I. and Kaercher, B.: Process-oriented large-eddy simulations of a midlatitude cirrus cloud system based on observations, Q. J. Roy. Meteor. Soc., 137, 374–393, 2011.

Starr, D. O. C., Benedetti, A., Boehm, M., Brown, P. R. A., Gierens, K. M., Girard, E., Giraud, V., Jakob, C., Jensen, E., Khvorostyanov, V. I., Koehler, M., Lare, A., Lin, R.-F., Maruyama, K., Montero, M., Tao, W.-K., Wang, Y., and Wilson, D.: Comparison of cirrus cloud models: a project of the GEWEX Cloud System Study (GCSS) working group on cirrus cloud system. Proceedings of the 13th International Conference on Cloud and Precipitation (ICCP), Reno, NV, USA, 14–18 August 2000.

Vosper, S. B.: Development and testing of a high resolution mountainwave forecasting system, Met. Apps., 10, 75–86, 2003.

Vosper, S. B. and Worthington, R. M.: Vhf radar measurements and model simulations of mountain waves wver wales, Q. J. Roy. Met. Soc., 128, 185–204, 2002.

Yang, H., Dobbie, S., Herbert, R., Connolly, P., Gallagher, M., Ghosh, S., Al-Jumur, S. M. R. K., and Clayton, J.: The effect of observed vertical structure, habits, and size distributions on the Solar radiative properties and cloud evolution of cirrus clouds, doi:10.1002/qj.973, 2012.

Zhang, M. H. and Lin, J. L.: Constrained variational analysis of sounding data based on column-integrated budgets of mass, heat, moisture, and momentum: Approach and application to arm measurements, J. Atmos. Sci., 54, 1503–1524, 1997.

Zhang, M. H., Lin, J. L., Cederwall, R. T., Yio, J. J., and Xie, S. C.: Objective analysis of arm iop data: Method and sensitivity, Mon. Wea. Rev., 129, 295–311, 2000.